Correlation effects in the electronic structure of $SrRuO_3$

J. Okamoto, T. Mizokawa, and A. Fujimori
Department of Physics, University of Tokyo, Bunkyo-ku, Tokyo 113-0033, Japan

I. Hase
Electrotechnical Laboratory, Umezono, Tsukuba 305-0801, Japan

M. Nohara and H. Takagi
Institute for Solid State Physics, University of Tokyo, Minato-ku, Tokyo 106-0032, Japan

Y. Takeda
Department of Chemistry, Faculty of Engineering, Mie University, Tsu 514-0008, Japan

M. Takano
Institute for Chemical Research, Kyoto University, Uji, Kyoto 611-0011, Japan
(Received 22 December 1998)

We have measured photoemission and inverse-photoemission spectra of the ferromagnetic metal $SrRuO_3$. The observed Ru $4d$-derived conduction band above and below the Fermi level (E_F) is found to be widely spread and the emission intensity at E_F to be weakened compared to band-structure calculations. Here, the calculations have been made for the ferromagnetic state with the actual distorted perovskite structure. We compare the spectra with the spectral density of states (DOS) obtained by modifying the band DOS with a phenomenological self-energy correction, which is chosen to be compatible with the measured electronic specific heat coefficient γ. Although the mass enhancement factor is only moderately large, ~ 4.4, the renormalization factor Z is found to be as small as ~ 0.08 ($Z^{-1} \sim 13$). These indicate a significant momentum dependence of the self-energy and a highly incoherent metallic state in $SrRuO_3$. We have also compared the photoemission and inverse-photoemission spectra taken below and above the Curie temperature, but significant changes have not been identified. [S0163-1829(99)01928-1]

I. INTRODUCTION

$3d$ transition-metal oxides have attracted much attention and have been studied in the past few decades because they show a variety of interesting electronic and magnetic properties. Because the $3d$ orbitals are rather localized, the $3d$ electrons feel strong Coulomb repulsion from each other. This strong Coulomb repulsion and resulting electron-electron correlation play essential roles in realizing the interesting physical properties such as antiferromagnetism, ferromagnetism, metal-insulator transition, and high-temperature superconductivity.[1]

The $4d$ orbitals in $4d$ transition-metal oxides are more extended than the $3d$ orbitals in $3d$ transition-metal oxides. It is therefore considered that the $4d$ electrons feel weaker Coulomb repulsion and that electron correlation is less important in $4d$ transition-metal oxides, making band theoretical descriptions more appropriate. So far, however, this point has not been sufficiently clarified because relatively few studies have been made on $4d$ transition-metal oxides. Indeed, some $4d$ transition-metal oxides exhibit such interesting physical properties as the unconventional superconductivity in Sr_2RuO_4,[2] and the metal-semiconductor transition in the pyrochlore-type $Tl_2Ru_2O_7$,[3] implying important roles of electron correlation.

$SrRuO_3$ is metallic and shows ferromagnetism below $T_C \simeq 160$ K.[4] According to the ionic picture, its electronic configuration is $4d^4$ in the low-spin $S=1$ state: the effective moment above T_C ($\sim 2.6\mu_B$/Ru)[5] agrees well with that of the low-spin Ru^{4+} ion ($2.83\mu_B$/Ru). It has an orthorhombically distorted perovskite structure of the $GdFeO_3$ type.[6] The resistivity shows an anomaly at T_C, indicating that spin fluctuations affect the transport properties.[7] Optical studies have shown characteristic behavior predicted for a Mott-Hubbard system[8] and the highly incoherent nature of conduction electrons.[9] The unusually high room-temperature resistivity, which well exceeds the Ioffe-Regel limit, was taken as a manifestation of the incoherent metallic state.[7]

Photoemission spectroscopy is a powerful technique to investigate the electronic structure of a correlated electron system.[1] More than a decade ago, Cox *et al.*[10] made a systematic ultraviolet photoemission study of Ru oxides including $SrRuO_3$, and interpreted the spectra based on multiplet theory. In a previous work, we measured the photoemission and O $1s$ x-ray absorption (XAS) spectra of $SrRuO_3$ and compared them to a band-structure calculation.[11] The photoemission spectra in the Ru $4d$ band region showed strong deviation from the band-structure calculation, indicating strong correlation effects, whereas the XAS spectrum agreed rather well with the calculation. In this work, we have measured high-resolution photoemission and inverse-photoemission spectra of $SrRuO_3$ and compared them to a band-structure calculation on the distorted crystal structure in order to obtain further information about its electronic struc-

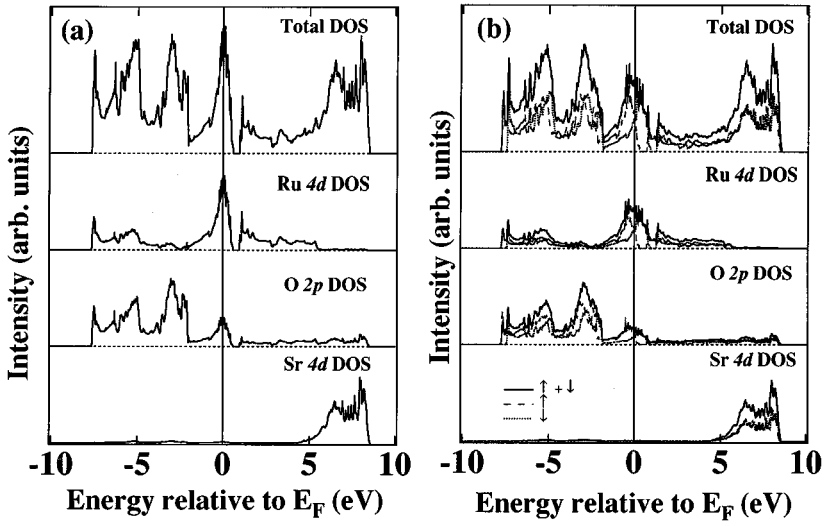

FIG. 1. Density of states of $SrRuO_3$ in the paramagnetic (a) and ferromagnetic (b) states obtained from L(S)DA band-structure calculations. The broken and dotted curves in (b) show the majority- and minority-spin states, respectively.

ture. We have also made specific heat measurements and analyzed the thermodynamic and spectroscopic data in a consistent way in a phenomenological self-energy approach.[12,13]

II. EXPERIMENT

Polycrystalline samples of $SrRuO_3$ were prepared by the following procedure. A mixture of RuO_2 and $SrCO_3$ powders was prefired at 1000 °C for 20 h in air. Then the mixture was pressed into a pellet and fired again at 1200 °C for 20 h in air. The product was milled and pressed into a pellet again ($\sim$2000 kg/cm^2). After firing at 1400 °C for 20 h in air, we obtained the $SrRuO_3$ polycrystals.

Photoemission spectroscopy (PES) measurements were carried out with the use of a He discharge lamp (He I: $h\nu = 21.2$ eV, He II: $h\nu = 40.8$ eV). The total resolution was $\sim$30 meV for He I and $\sim$50 meV for He II and the base pressure in the spectrometer was $\sim 10^{-10}$ Torr. The samples were cooled using a He refrigerator down to $\sim$50 K. We scraped the sample surfaces in the ultrahigh vacuum at low temperatures with a diamond file. We checked the surface condition by monitoring the emission at ~ -9 eV below the Fermi level (E_F), which is known due to contamination or surface degradation. Although we could not totally eliminate that emission, we kept its intensity to the minimum level and repeated scraping before its intensity grew. In this sense, the present method was successful in preparing clean surfaces of the oxides compared to annealing in an oxygen atmosphere employed by Cox *et al.*[10] The calibration of binding energies was achieved by measuring the Fermi edge of Au evaporated on the samples. Inverse-photoemission spectra were taken in the bremsstrahlung-isochromat spectroscopy (BIS) mode. Photons with the energy of 1486.6 eV were detected using a SiO_2 multicrystal monochrometer. The energy resolution was $\sim$0.8 eV, and the base pressure was in the 10^{-10} Torr range. The calibration of energies was also achieved by measuring the Fermi edge of Au evaporated on the samples. XAS spectra from the O 1*s* core level were measured in the total electron-yield mode at beam line 2B of the Photon Factory, High Energy Accelerator Research Organization. The energy resolution was $\sim$0.2 eV and the base pressure was $\sim 10^{-10}$ Torr. Photon energies were calibrated using the O 1*s* absorption peak of TiO_2 at 530.7 eV and the Cu $2p_{3/2}$ absorption peak at 932.5 eV. During the BIS and O 1*s* XAS measurements, we paid attention to a slope around 5 eV above E_F, which was a sign of degradation or contamination of the sample. As in the case of the PES measurements, we scraped the samples *in situ* with a diamond file until the slope disappeared. The spectra were taken at liquid-nitrogen temperature ($\sim$80 K) for both the BIS and O 1*s* XAS measurements.

For the low temperature specific-heat measurements, we employed the thermal relaxation method.[14] A polycrystalline sample of 11.45 mg was measured without external field between 1.4 K and 20 K.

III. BAND-STRUCTURE CALCULATION

The band structure was calculated for the orthorhombically distorted structure of $SrRuO_3$ using the local-spin-)density approximation [L(S)DA]. The calculated band density of states (DOS) $N_b(\omega)$ in the ferromagnetic state as well as that in the paramagnetic state are shown in Fig. 1. The Ru $4d$ t_{2g} band around E_F shows an exchange splitting in the ferromagnetic state and thus is broadened compared to that in the paramagnetic state. Because of the orthorhombic distortion, the Ru $4d$ band DOS is not narrow enough to be split into two peaks in the ferromagnetic state as in the previous calculation,[11] in agreement with a recent band-structure calculation by Santi and Jarlborg.[15] The total ferromagnetic moment was obtained as 1.52 μ_B and the magnetic moment at the Ru site as 0.97 μ_B. These values are smaller than those predicted by Santi and Jarlborg (2.0 and 1.6 μ_B, respectively)[15] and are compared with the experimental values: 1.4 μ_B from neutron diffraction,[16] 1.1 μ_B from the magnetization in 1.67 T at 4.2 K,[17] and 1.27 μ_B from the magnetization in 5.5 T at 6 K.[18]

IV. RESULTS AND DISCUSSIONS

We compare the measured spectra with the band-structure calculations in Fig. 2. The band DOS has been broadened

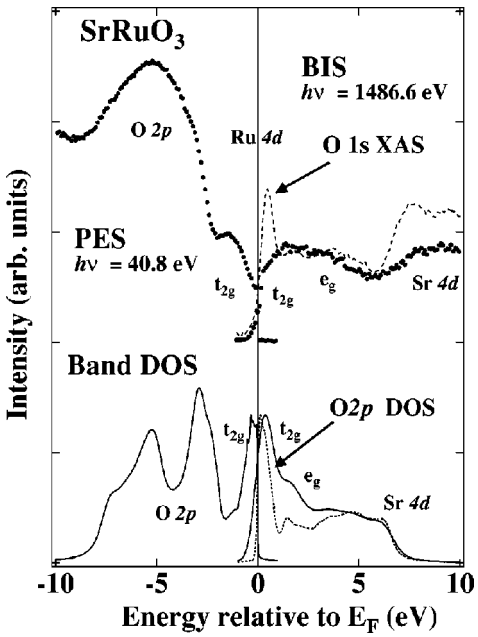

FIG. 2. PES, BIS, and O 1*s* XAS spectra of $SrRuO_3$ compared to the band DOS in the ferromagnetic state. The calculated DOS has been broadened with a Gaussian (50 meV FWHM for PES and 0.8 eV FWHM for BIS) and a Lorentzian (FWHM$=0.1|E-E_F|$) function. For comparison with the XAS spectrum, the oxygen $2p$ DOS is plotted on the same scale broadened with a Gaussian (0.2 eV FWHM) and the Lorentzian.

with a Gaussian and a Lorentzian function for the instrumental resolution and the lifetime broadening, respectively. As shown in the previous work,[11] the band-structure calculations indicate that the band between ~ 5 eV to ~ -2 eV measured relative to E_F is mainly composed of Ru $4d$ character and that between ~ -2 to ~ -10 eV is mainly of O $2p$ character. The measured O $2p$ band shows less pronounced structures than the calculations. The empty Sr $4d$ states in the BIS and XAS spectra appear at higher energies than the calculated DOS. The O 1*s* XAS spectrum, which probes the unoccupied O $2p$ DOS, agrees well with that reported in the previous work:[11] the O 1*s* XAS spectrum reflects the sharp structure of the unoccupied t_{2g} states just above E_F. For the XAS spectrum, however, the effects of the core-hole potential cannot be ignored and the spectrum does not actually represent the single-particle excitation spectrum. On the other hand, the Ru $4d$ band in the PES and BIS spectra represent the single-particle excitation spectra but do not agree with the band DOS. In the measured spectra, the d band structure is much broader and the intensity at E_F is much weaker than the band DOS.

From these results, we consider that the sharp peaks near E_F in the band DOS originating from the t_{2g} band are modified by the effect of electron correlation in the PES and BIS spectra. In the present work, we follow the previous assignment[11] that the Fermi-edge emission and the broad band at ~ -1.2 eV peak are due to the coherent and incoherent parts of the spectral function, respectively, as in the photoemission spectra of Ti and V oxides.[12,19,20] The BIS spectrum shows a line shape similar to the PES spectrum and the similar interpretation appears to be possible. The coherent part represents quasiparticle excitations with **k** dispersions and reflects the itinerancy of the $4d$ electrons, whereas the incoherent part represents the remanent of the lower and upper Hubbard bands and reflects localized excitations. Cox *et al.*[10] interpreted the coherent part as the minority-spin states of the t_{2g} band and the incoherent part as the majority-spin states based on the multiplet analysis of the paramagnetic semiconductor $Y_2Ru_2O_7$. In the XAS spectrum the correlation effect is probably canceled by the core-hole effects. The separation between the coherent and incoherent parts in the present case is, however, not so distinct as in the case of Ti and V oxides and will not be stressed here. Instead, we will mainly consider the effective mass deduced from the DOS at E_F and the electronic specific heat. As for the spectral line shape, we will utilize the self-energy correction to the band DOS.

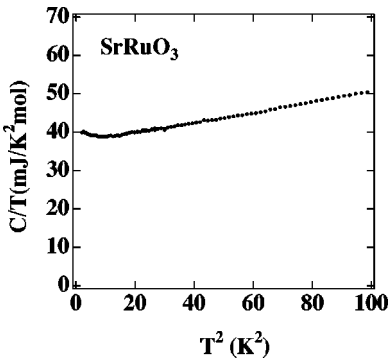

FIG. 3. Specific heat of $SrRuO_3$ plotted in C/T versus T^2.

Figure 3 shows the specific heat data below 10 K plotted in C/T vs T^2. The data are fitted by the formula $C/T=\gamma+\beta T^2$, where $\beta \propto 1/\Theta_D^3$ and γ is the electronic specific heat coefficient. From a least-square fitting procedure, we have estimated $\gamma=36.3$ mJ/K^{2}mol and the Debye temperature $\Theta_D=364$ K. Allen *et al.*[21] obtained nearly the same $\Theta_D=368$ K and a little smaller $\gamma=30$ mJ/K^{2}mol. γ is given by the band DOS $N_b(\omega)$ at E_F, $\gamma=\gamma_b(m^*/m_b)$, where $\gamma_b=(\pi^2/3)k_B^2N_b(E_F)$, m_b is the bare band mass and m^* is the effective mass. If electron correlation is not negligible, γ obtained from the specific heat is different from that estimated from the band DOS, $\gamma_b=7.16$ mJ/K^{2}mol. The ratio between γ and γ_b yields the mass enhancement factor m^*/m_b, which is found to be 4.43 in the present work. Allen *et al.* deduced a smaller value of 3.7.[21]

We have attempted to simulate the observed Ru $4d$ band spectra by applying a phenomenological self-energy correction $\Sigma(\mathbf{k},\omega)$ to the ferromagnetic band DOS. We have imposed the constraint that the self-energy retains the Fermi-liquid properties [$\mathrm{Im}\,\Sigma(\mathbf{k},\omega)\propto-\omega^2$ near $\omega=0$] and that the effective mass calculated from the band mass and self-energy coincides with the thermal effective mass. The **k** dependence of the self-energy reduces the spectral DOS at E_F by the reduction factor,[19]

$$\frac{m_k}{m_b}\equiv\left|\frac{\partial\varepsilon_{\mathbf{k}}}{\partial\mathbf{k}}\right|\Bigg/\left|\frac{\partial\varepsilon_{\mathbf{k}}}{\partial\mathbf{k}}+\frac{\partial\,\mathbf{Re}\,\Sigma(\mathbf{k},\omega)}{\partial\mathbf{k}}\right|_{\omega=0,\mathbf{k}=\mathbf{k}_F}, \qquad (1)$$

where m_k is called the **k** mass. From comparison between the band DOS and the PES and BIS spectra shown in Fig. 2, m_k/m_b is estimated to be ~ 0.4. The spectral weight of the

coherent part is given by the renormalization factor $Z \equiv \{1 - [\partial \mathbf{Re}\,\Sigma(\mathbf{k},\omega)/\partial\omega]|_{\omega=0,\mathbf{k}=\mathbf{k}_F}\}^{-1}$. The lost spectal weight $1-Z$ is distributed in the incoherent part centered at ~ -1.2 eV.

For simplicity, we have assumed that $\Sigma(\mathbf{k},\omega)$ is decomposed into a $\mathbf{k}$-dependent part and a ω-dependent part of the simple form:[22]

$$\Sigma(\mathbf{k},\omega) = \frac{g_1\omega}{(\omega+i\Gamma_1)^2} - g_2\left(\frac{1}{\omega+i\Gamma_2}+\frac{i}{\Gamma_2}\right) + \frac{2U}{\pi V}\arctan\left(\frac{\varepsilon_{\mathbf{k}}}{V}\right), \quad (2)$$

where g_1, Γ_1, g_2, Γ_2, U, and V are adjustable parameters, which are to be determined so that the self-energy-corrected DOS agrees well with the experimental spectra under the condition that the calculated effective mass agrees with the electronic specific heat coefficient γ. The first and second terms in Eq. (2) represent local and dynamical effects and cause the band narrowing of the coherent part and spectral weight transfer from near E_F ($\omega \equiv 0$) to away from E_F. The first term in Eq. (2) gives rise to incoherent features away from E_F while the second term contributes extra broadening to the incoherent features. The third term in Eq. (2) represents the nonlocal effects and uniformly broadens the band near E_F. We have neglected the spin dependence of the self-energy, for simplicity. The effective mass m^*, which is proportional to the quasiparticle density at E_F, is given by $m^*/m_b = Z^{-1}(m_{\mathbf{k}}/m_b) \simeq (1+g_1/\Gamma_1^2+g_2/\Gamma_2^2)(1+2U/\pi V^2)^{-1}$. A similar analysis has been made for the spectra of the superconductor Sr_2RuO_4, and strong electron correlation effects have been found.[23]

Figure 4 shows the best fit result of the self-energy-corrected ferromagnetic DOS using parameter values, $g_1 = 0.11$ eV^2, $\Gamma_1 = 0.1$ eV, $g_2 = 0.0049$ eV^2, $\Gamma_2 = 0.07$ eV, $U = 1.5$ eV^2, and $V = 0.7$ eV. The energy-dependent part of the self-energy for these parameters are shown in the bottom of Fig. 4. The broken curves in Fig. 4 show the tail of the O $2p$ band and the integral background (determined between 0 and -9 eV) in the PES spectrum, and that of the e_g band and the integral background (determined between 0 and 6 eV) in the BIS spectrum. The dotted curves in Fig. 4 are the sum of the broken curves in each spectrum. Here, we have decomposed the Ru $4d$ DOS into the narrow t_{2g} band and wide e_g band and assumed that electron correlation is important only for the t_{2g} part.[24] From the above parameter set, we have obtained $Z^{-1} = 13$, $m_{\mathbf{k}}/m_b = 0.34$, and the mass enhancement factor $m^*/m_b = 4.5$. Although Z^{-1} is large, the effect of the $\mathbf{k}$ mass reduces the effective mass. Nearly the same values were obtained for Sr_2RuO_4: $Z^{-1} = 11.1$, $m_{\mathbf{k}}/m_b = 0.40$, and $m^*/m_b = 4.43$.[23] Hence we conclude that the effect of electron correlation cannot be ignored in the electronic structure of the Ru $4d$ states in $SrRuO_3$ as well as in Sr_2RuO_4.

Finally, we compare in Fig. 5 the PES and BIS spectra taken above and below T_C. The spectra taken at different temperatures, which have been normalized to the integrated area within the indicated energy ranges, have not shown clear temperature-dependent changes. This means that the anomaly in the resistivity at T_C is not attributed to the changes in the number of carries but to the spin fluctuations.[7] This observed temperature dependence is different from that observed for the double exchange systems $La_{1-x}Sr_xMnO_3$,[25,26] and $La_{1-x}Ca_xMnO_3$,[27] and from band-structure calculations as shown in Fig. 1. This implies that the ferromagnetism in $SrRuO_3$ is not explained simply by the double exchange ferromagnetism nor by itinerant-electron ferromagnetism based on band theory.

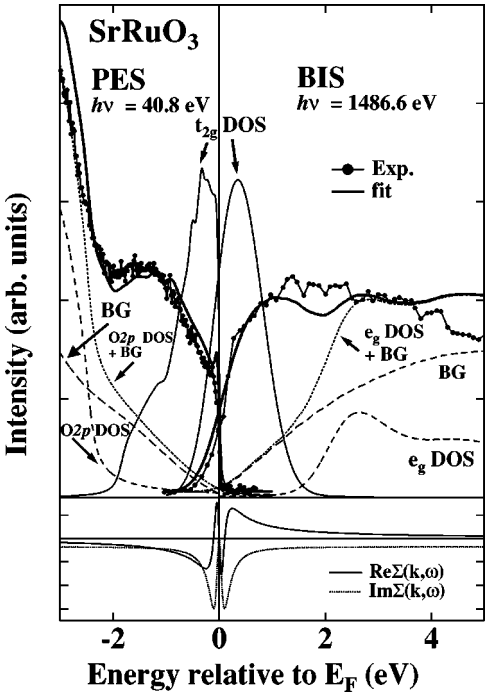

FIG. 4. PES and BIS spectra compared with the theoretical fit using the self-energy-corrected DOS in the region near the Fermi level. The fitted curves have been obtained by summing the self-energy-corrected Ru $4d$ t_{2g} band DOS, the O $2p$ nonbonding band DOS (the Ru $4d$ e_g band DOS) and the integral background for the PES (BIS) spectrum. The bottom panel shows the energy-dependent part of the self-energy used to fit the spectra.

V. CONCLUSION

We have measured the PES, BIS, and O $1s$ XAS spectra of $SrRuO_3$ in the ferromagnetic state. By comparing the band

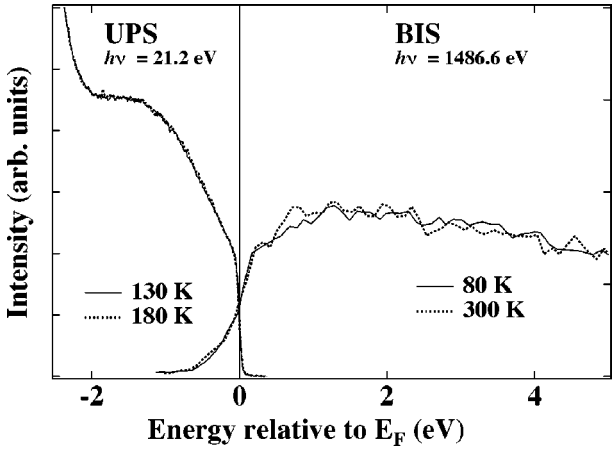

FIG. 5. PES and BIS spectra taken above and below the Curie temperature $T_C \simeq 160$ K.

DOS with these spectra, we have found that the effect of electron correlation is substantial in the Ru $4d\ t_{2g}$ states of $SrRuO_3$: in the PES and BIS measurements, which represent the single-particle excitation spectra, the spectra do not agree well with the band DOS, especially in the region near E_F. We have compared the PES and BIS spectra with the DOS modified by the self-energy correction. Although the Z^{-1} is large, the effective mass is relatively small, ~ 4.4, owing to the **k** mass. The modified DOS curves can be fitted to the PES and BIS spectra. The temperature dependence of the PES and BIS spectra of $SrRuO_3$ is found to be weak, indicating that the ferromagnetism in $SrRuO_3$ is different from the double exchange ferromagnetism in the Mn oxides and from itinerant-electron ferromagnetism based on band theory.

ACKNOWLEDGMENTS

We thank A. Sekiyama, K. Kobayshi, K. Mamiya, T. Konishi, and the staff of the Photon Factory for technical support, and M. Izumi for useful discussions. This work was supported by a Special Coordination Fund for Promoting Science and Technology from the Science and Technology Agency of Japan and by the New Industrial Technology Development Organization (NEDO). The work at the Photon Factory was made under the approval of the Photon Factory Program Advisory Committee (Proposal No. 94G361).

[1] See, e.g., M. Imada, A. Fujimori, and Y. Tokura, Rev. Mod. Phys. **70**, 1039 (1998).
[2] Y. Maeno, H. Hashimoto, K. Yoshida, S. Nishizaki, T. Fujita, J. G. Bednortz, and F. Lichtenberg, Nature (London) **372**, 532 (1994).
[3] A. W. Sleight and J. L. Gillson, Mater. Res. Bull. **6**, 781 (1971).
[4] T. Yamamoto, R. Kanno, Y. Takeda, O. Yamamoto, Y. Kawamoto, and M. Takano, J. Solid State Chem. **109**, 372 (1994).
[5] A. Callaghan, C. W. Moeller, and R. Ward, Inorg. Chem. **5**, 1573 (1966).
[6] R. J. Bouchard and J. L. Gillson, Mater. Res. Bull. **7**, 873 (1972).
[7] L. Klein, J. S. Dodge, C. H. Ahn, G. J. Snyder, T. H. Geballe, M. R. Beasley, and A. Kapitulnik, Phys. Rev. Lett. **77**, 2774 (1996).
[8] J. S. Ahn, J. Bak, H. S. Choi, T. W. Noh, J. E. Han, Yunkyu Bang, J. H. Cho, and Q. X. Xia, cond-mat/9807209 (unpublished).
[9] P. Kostic, Y. Okada, N. C. Collins, Z. Schlesinger, J. W. Reiner, L. Klein, A. Kapitulnik, T. H. Geballe, and M. R. Beasley, Phys. Rev. Lett. **81**, 2498 (1998).
[10] P. A. Cox, R. G. Egdell, J. B. Goodenough, A. Hamnett, and C. C. Naish, J. Phys. C **16**, 6221 (1983).
[11] K. Fujioka, J. Okamoto, T. Mizokawa, A. Fujimori, I. Hase, M. Abbate, H. J. Lin, C. T. Chen, Y. Takeda, and M. Takano, Phys. Rev. B **56**, 6380 (1997).
[12] I. H. Inoue, I. Hase, Y. Aiura, A. Fujimori, Y. Haruyama, T. Maruyama, and Y. Nishihara, Phys. Rev. Lett. **74**, 2539 (1995).
[13] I. H. Inoue, I. Hase, Y. Aiura, A. Fujimori, K. Morikawa, Y. Haruyama, T. Maruyama, and Y. Nishikawa, Physica C **235-240**, 1007 (1994).
[14] G. R. Stewart, Rev. Sci. Instrum. **54**, 1 (1983).
[15] G. Santi and T. Jarlborg, J. Phys.: Condens. Matter **9**, 9563 (1997).
[16] J. M. Longo, P. M. Raccah, and J. B. Goodenough, J. Appl. Phys. **39**, 1327 (1968).
[17] A. Kanbayshi, J. Phys. Soc. Jpn. **41**, 1876 (1976).
[18] J. J. Neumeier, A. L. Cornelius, and J. S. Schilling, Physica B **198**, 324 (1994).
[19] K. Morikawa, T. Mizokawa, K. Kobayashi, A. Fujimori, H. Eisaki, S. Uchida, F. Iga, and Y. Nishihara, Phys. Rev. B **52**, 13 711 (1995).
[20] A. Fujimori, I. Hase, H. Namatame, Y. Fujishima, Y. Tokura, H. Eisaki, S. Uchida, K. Takegahara, and F. M. F. de Groot, Phys. Rev. Lett. **69**, 1796 (1992).
[21] P. B. Allen, H. Berger, O. Chauvet, L. Forro, T. Jarlborg, A. Junod, B. Revaz, and G. Santi, Phys. Rev. B **53**, 4393 (1996).
[22] T. Saitoh, A. Sekiyama, T. Mizokawa, A. Fujimori, K. Ito, H. Nakamura, and M. Shiga, Solid State Commun. **95**, 307 (1995).
[23] I. H. Inoue, Y. Aiura, Y. Nishihara, Y. Haruyama, S. Nishizaki, Y. Maeno, T. Fujita, J. G. Bednortz, and F. Lichtenberg, Physica B **223&224**, 516 (1996);I. H. Inoue, Y. Aiura, Y. Nishihara, Y. Haruyama, S. Nishizaki, Y. Maeno, T. Fujita, J.G. Bednortz, and F. Lichtenberg, J. Electron Spectrosc. Relat. Phenom. **78**, 175 (1996).
[24] H. F. Pen, M. Abbate, A. Fujimori, Y. Tokura, H. Eisaki, S. Uchida, and G. A. Sawatzky, Phys. Rev. B **59**, 7422 (1999).
[25] D. D. Sarma, N. Shanthi, S. R. Krishnakumar, T. Saitoh, T. Mizokawa, A. Sekiyama, K. Kobayashi, A. Fujimori, E. Weschke, R. Meier, G. Kaindl, Y. Takeda, and M. Takano, Phys. Rev. B **53**, 6873 (1996).
[26] T. Saitoh, A. Sekiyama, K. Kobayashi, T. Mizokawa, A. Fujimori, D. D. Sarma, Y. Takeda, and M. Takano, Phys. Rev. B **56**, 8836 (1997).
[27] J.-H. Park, C. T. Chen, S-W. Cheong, W. Bao, G. Meigs, V. Chakarian, and Y. U. Idzerda, Phys. Rev. Lett. **76**, 4215 (1996).